AFRL-RW-EG-TP-2008-7407

RE-VISITING 1-D HYPERVELOCITY PENETRATION (PREPRINT)

David E. Lambert (AFRL/RWMW)
Damage Mechanisms Branch
Air Force Research Laboratory
Munitions Directorate
Eglin AFB, FL   32542

APRIL 2008

JOURNAL ARTICLE (PREPRINT)

AIR FORCE RESEARCH LABORATORY, MUNITIONS DIRECTORATE

■ **Air Force Material Command**　　■ **United States Air Force**　　■ **Eglin Air Force Base**

REPORT DOCUMENTATION PAGE

The public reporting burden for this collection of information is estimated to average 1 hour per response, including the time for reviewing instructions, searching existing data sources, gathering and maintaining the data needed, and completing and reviewing the collection of information. Send comments regarding this burden estimate or any other aspect of this collection of information, including suggestions for reducing the burden, to Department of Defense, Washington Headquarters Services, Directorate for Information Operations and Reports (0704-0188), 1215 Jefferson Davis Highway, Suite 1204, Arlington, VA 22202-4302. Respondents should be aware that notwithstanding any other provision of law, no person shall be subject to any penalty for failing to comply with a collection of information if it does not display a currently valid OMB control number.
PLEASE DO NOT RETURN YOUR FORM TO THE ABOVE ADDRESS.

1. REPORT DATE *(DD-MM-YYYY)*	2. REPORT TYPE	3. DATES COVERED *(From - To)*

4. TITLE AND SUBTITLE

5a. CONTRACT NUMBER

5b. GRANT NUMBER

5c. PROGRAM ELEMENT NUMBER

6. AUTHOR(S)

5d. PROJECT NUMBER

5e. TASK NUMBER

5f. WORK UNIT NUMBER

7. PERFORMING ORGANIZATION NAME(S) AND ADDRESS(ES)

8. PERFORMING ORGANIZATION REPORT NUMBER

9. SPONSORING/MONITORING AGENCY NAME(S) AND ADDRESS(ES)

10. SPONSOR/MONITOR'S ACRONYM(S)

11. SPONSOR/MONITOR'S REPORT NUMBER(S)

12. DISTRIBUTION/AVAILABILITY STATEMENT

13. SUPPLEMENTARY NOTES

14. ABSTRACT

15. SUBJECT TERMS

16. SECURITY CLASSIFICATION OF:			17. LIMITATION OF ABSTRACT	18. NUMBER OF PAGES	19a. NAME OF RESPONSIBLE PERSON
a. REPORT	b. ABSTRACT	c. THIS PAGE			19b. TELEPHONE NUMBER *(Include area code)*

Re-visiting 1-D Hypervelocity Penetration

D. E. Lambert

Air Force Research Laboratory, Munitions Directorate
101 W. Eglin Blvd., Suite 135, Eglin Air Force Base, FL 32542, USA

Abstract

Classical, one-dimensional theory of hydrodynamic penetration is used as the basis of establishing simplified analytical relationships describing energy, momentum, and power deposition during hypervelocity impact events. A concise overview of the 1-D model is given followed by a select grouping of terms into relationships that offer first-order criteria for making engineering design considerations on relevant applications and assist in the analysis of experimental observations. Momentum, energy, and power deposition are found to be proportional to second, third and fourth power exponents, respectively. These analytical terms are presented for constant velocity gradient, i.e. fixed length, rods as well as linear velocity gradient rods, such as shaped charge jets.

The role of penetrator-to-target density ratio is then examined in terms of the backflow, or reverse flow of 1-D penetration. Again, the non-dimensional ratio of penetrator-to-target mass density is used to compare the relative velocity of material flow during penetration. The relationship highlights the role of penetrator materials for achieving desired effects in these hypervelocity, terminal ballistics events.

Albeit the relationships are derived on the assumptions for hydrodynamic processes, their generality of form and ease of implementation make them a useful first-order description for engineering insight and application over a broad range of velocities.

Keywords: Hypervelocity Penetration, Energy Deposition of Jets, Reverse Flow, Shaped Charge Warhead

1. INTRODUCTION

The Bernoulli equation has long been used to produce simplified, but insightful analytical relationships for such useful terms as the penetration depth, penetrator erosion rate, and interface velocity of the penetrator-target for hypervelocity and shaped charge jet impacts [1,2]. Further efforts [3,4] expanded on the fundamental equations to establish relationships of energy and momentum flux and deposition rates for constant velocity and linear velocity gradient rods. The work of Foster and Wilson serves as the foundation of the derivations within this paper. A brief review of the basic equations is necessary for completeness and establishing variations of the forms for further study and discussion.

1.1 The Case of a Constant Velocity Rod

Derivations are first made for a constant velocity rod. The Bernoulli equation, with its assumption of incompressible and inviscid conditions, is applied along the centerline of a hypervelocity projectile impacting a target, Figure 1.

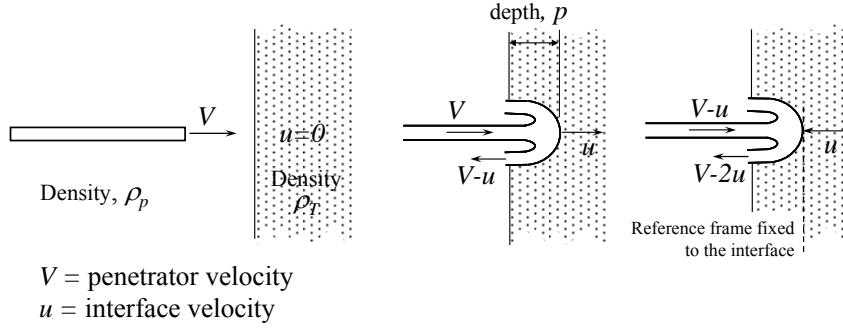V = penetrator velocity
u = interface velocity

Fig. 1. Penetration terminology.

The steady-state assumption is most easily understood in the reference frame being fixed to the penetrator/target interface, giving the streamline energy equality and solution, Equation (1).

$$\tfrac{1}{2}\rho_P(V-u)^2 = \tfrac{1}{2}\rho_T u^2 \quad \text{having interface velocity} \quad u = \frac{V}{1+\gamma} \tag{1}$$

With term γ defined for the square root of the ratio of target density to penetrator density. The rate of erosion of the rod increment, dl/dt, and the rate of penetration (advancement of the interface), dp/dt, are,

$$\frac{dl}{dt} = V - u \;\Rightarrow\; \frac{dl}{dt} = \frac{V\gamma}{1+\gamma} \tag{2}$$

Using the differential chain rule, the increment in penetration per unit rod length consumed is also found in terms of γ, knowing that the interface velocity is also $u = dp/dt$,

$$\frac{dp}{dt}\frac{dt}{dl} = \left(\frac{V}{1+\gamma}\right)\left(\frac{1+\gamma}{V\gamma}\right) \Rightarrow \frac{dp}{dl} = \frac{1}{\gamma} \tag{3}$$

The momentum, $\bar{p}$, and energy, E, terms are defined for the constant velocity rod having a fixed cross-sectional area, A.

$$\bar{p} = \rho_p AlV \quad \text{and} \quad E = \tfrac{1}{2}\rho_p AlV^2 \tag{4}$$

Again, the chain rule is used to find the momentum and energy deposited per unit penetration path

length, as well as the power density of the impacting rod,

$$\frac{d\overline{p}}{dp} = \frac{d\overline{p}}{dl}\frac{dl}{dp} = \rho_p A V \gamma \tag{5}$$

$$\frac{dE}{dp} = \frac{dE}{dl}\frac{dl}{dp} = \tfrac{1}{2}\rho_p A V^2 \gamma$$

$$\frac{dP}{dA} = \frac{dE}{dtdA} = \frac{dE}{dl}\frac{dl}{dt} = \tfrac{1}{2}\rho_p V^3 \frac{\gamma}{1+\gamma}$$

1.2 The Case of a Linear Velocity Rod

The derivation of penetration relationships for the linear velocity gradient penetrator, described in Figure 2, is now given. This domain is suitable for idealized penetration descriptions of shaped charge jets solved in its virtual coordinate frame [5].

The velocity of the penetration interface at any time after impact is, $u = dx/dt$, with the position of the penetrator being generally described by the ever-changing, eroding tip velocity in the target as,

$$x = Vt \tag{6}$$

A non-dimensional position response is obtained by integrating the penetration interface relation with substitutions of Eq. (6) and recalling that $u = dp/dt = V/(1+\gamma)$ to get,

$$\frac{x}{x_0} = \left(\frac{t}{t_0}\right)^{\frac{1}{1+\gamma}} \tag{7}$$

Through judicious manipulation of Eq. (6) and substitution of Eq. (7), the velocity is obtained in terms of initial, known values and virtual origin coordinates,

$$V = \frac{x}{t} = \frac{x}{x_0}\frac{x_0}{t_0}\frac{t_0}{t} \quad \Rightarrow \quad V = V_0\left(\frac{x}{x_0}\right)^{-\gamma} \tag{9}$$

Here, the area is no longer a constant, but is a time-dependent parameter changing with length as governed by the velocity gradient between the leading tip and the tail mass points.

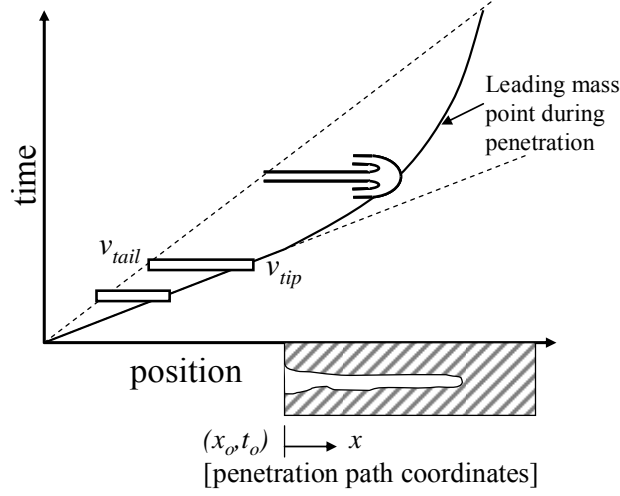$$A(t) = \frac{m_0}{\rho_p(V_{tip} - V_{tail})t} \tag{10}$$

Fig. 2. Linear velocity gradient rod penetration.

Time can be eliminated from the area relationship through the initial conditions,

$$\frac{1}{t_0} = \frac{V_{tip}}{x_0} \quad \text{and} \quad \frac{1}{t} = \frac{t}{t_0}\left(\frac{x}{x_0}\right)^{-(1+\gamma)} \tag{11}$$

Giving area as a function of spatial dependency, known quantities, and virtual coordinates,

$$A(x) = \frac{m_0 V_{tip}}{\rho_p (V_{tip} - V_{tail})x_0}\left(\frac{x}{x_0}\right)^{-(1+\gamma)} \tag{12}$$

Using the relationships derived for the constant velocity case, Eq. (5), and substituting for area, Eq. (12) and velocity, Eq. (9), the momentum and energy relationships deposited per unit penetration distance for the case of a linear velocity gradient penetrator are found as,

$$\frac{d\overline{p}}{dp} = \frac{\gamma\, m_0 V_{tip}^2}{(V_{tip} - V_{tail})x_0}\left(\frac{x}{x_0}\right)^{-(1+2\gamma)} \tag{13}$$

$$\frac{dE}{dp} = \frac{\gamma\, m_0 V_{tip}^3}{2(V_{tip} - V_{tail})x_0}\left(\frac{x}{x_0}\right)^{-(1+3\gamma)} \tag{14}$$

And the power input function is then,

$$\frac{dE}{dt} = \frac{m_0 V_{tip}^4}{2(V_{tip} - V_{tail})x_0} \left(\frac{\gamma}{1+\gamma}\right)\left(\frac{x}{x_0}\right)^{-(1+4\gamma)}$$

(15)

2. DISCUSSION OF THE 1-D RELATIONSHIPS

The momentum and energy relationships for both the constant and linear gradient velocity rods are similar enough in form to discuss interchangeably.

2.1 Constant Velocity Rod

The simpler case of the constant velocity rod is discussed first. Even though the power density is mainly dependent (third-power) on velocity, there is a non-linear contribution from penetrator material density. The plot of Figure 3 extracts the velocity-dependence and examines just the $\rho_p\gamma/(1+\gamma)$ term versus material density for rods penetrating a target of density $\rho_T = 7850$ kg/m^3, e.g. steel. The benefit of this input energy must be considered along with transmitted shock strength and efficiency as coupled by the Hugoniot match for the penetrator/target combination. There are target failure mechanisms, albeit not covered in such a simplistic 1-D theory, which might be activated using a rapid deposition of energy. Mechanisms of brittle fracture, pore collapse, spallation, phase change, and/or crush-up are but a few to consider the need for attaining high power density. Selection of penetrator density, velocity characteristics, and standoff of the velocity gradient rods are now available for parametric evaluation.

2.2 Linear Velocity Gradient Rod

The case of the linear velocity gradient penetrators presents a more interesting investigation. The gradient imposes standoff sensitivity of the penetration relationships. Additionally, the high velocity typically resulting from shaped charge jets is seen to significantly contribute to the momentum, energy and power. Less obvious, but of relevance to the discussions made herein, is the contribution of the material densities. The density ratio, γ, is found to contribute to the spatial terms of momentum, Eq. (13), to the 2nd power and energy, Eq. (14), to the 3rd power. An illustration for the energy deposition is given in Figure 4 for a linear velocity rod having mass of 0.1kg with leading tip velocity of 10km/s and tail velocity of 3km/s. Three different material densities are selected - aluminum, copper, and tungsten – to show how energy is deposited according to γ dependency.

The low density materials deposit their energy in the initial phase while the high density materials carry a greater percentage of their kinetic energy deeper into the target. For this example, the Al deposits over 2.5 times the energy than the U rod. Recognize that this is only an input quantity and does not account for post penetrator/target interface events or other complex target response mechanisms. However, the response curves are useful as a fundamental criterion or screening parameter for selecting a penetrator material to address a specific target material and/or penetration objective. One example is that a low density shaped charge liner material might be used to maximize the entrance hole area with shallow depth for mining purposes.
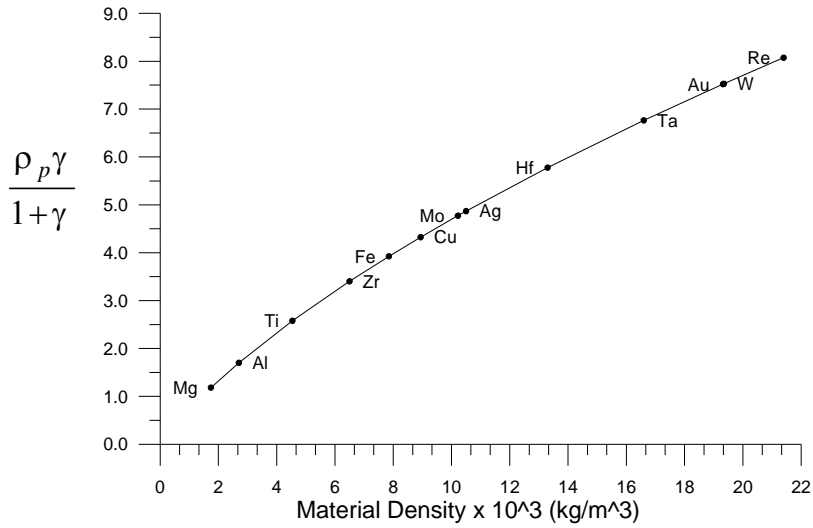
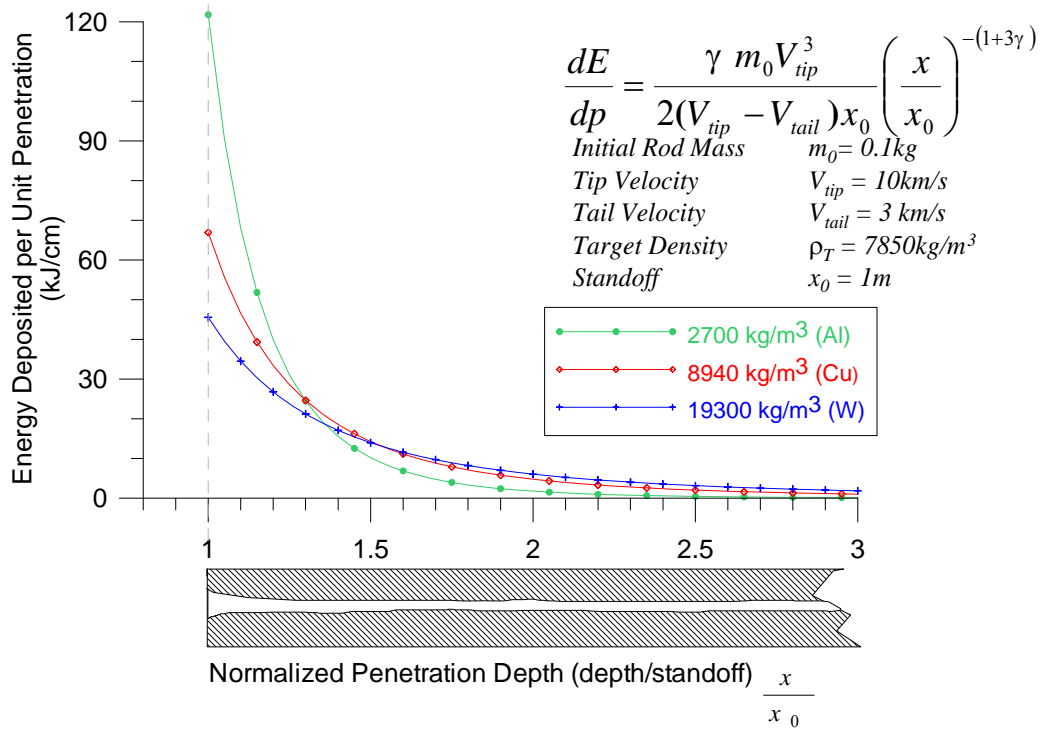Fig. 3. Density term of the power input, Eq. (5), for various rod materials penetrating a steel target.

$$\frac{dE}{dp} = \frac{\gamma \; m_0 V_{tip}^3}{2(V_{tip} - V_{tail})x_0}\left(\frac{x}{x_0}\right)^{-(1+3\gamma)}$$

Initial Rod Mass $m_0 = 0.1kg$
Tip Velocity $V_{tip} = 10km/s$
Tail Velocity $V_{tail} = 3 \; km/s$
Target Density $\rho_T = 7850kg/m^3$
Standoff $x_0 = 1m$

Fig. 4. Effect of penetrator density on energy deposition for a linear velocity gradient rod.

2.3 Energy Deposition of a Shaped Charge Jet

The effect of power deposition is made through an experiment of a shaped charge jet penetrating a finite thick, but severely over-matched piece of armor.   A 5-inch diameter, copper-lined warhead (typically used for very deep penetration) was fired against only a 6-inch thick armor plate at 3-charge diameter (CD) standoff. A radiograph of the jet at 150us is shown in Figure 5 with the tip traveling at 9.54 km/s. The high-degree of overmatch in target thickness versus its total penetration capability resulted in a violent, explosion-type, of target spallation as seen in Figure 6.   Following the 1-D analysis presented, Eq. (9), and the virtual origin approximations for this shaped charge design, the velocity of the eroded tip at the time it reaches the rear surface of the 6-inch target is 8.51 km/s. This segment of jet length has then proceeded through the 6-inches of steel with an input power deposition of 8.5 MW.

Photographs of the target plate from this hypervelocity penetration experiment are given in Figure 6. The rear surface has a noticeable square-ended cavity with the surface dominated by ductile dimple and pure tension features.   The rapid deposition of energy and the intense reflected shock from hypervelocity impact produced such severe and localized spallation event.
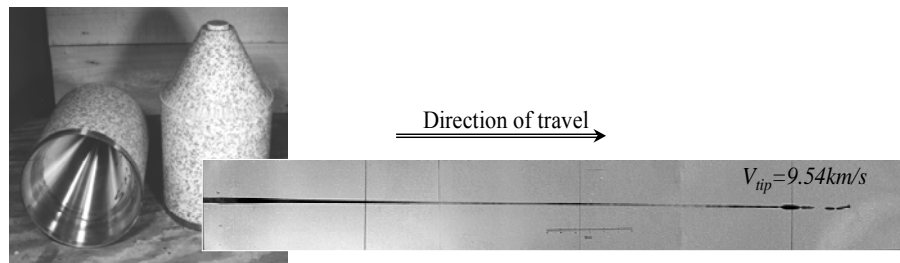

Fig. 5. Radiograph of a high velocity, copper liner shaped charge jet.
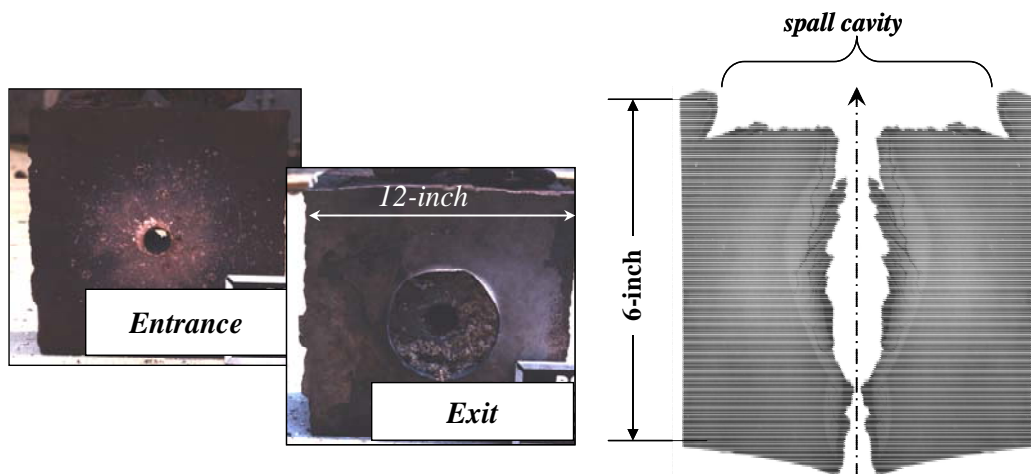

Fig. 6. Target of significant over-matched penetration event. Cross-section cut (far right) shows severity of spallation with power input of approx. 8.5MW.

2.4 Hole-Volume and Energy Relationship

Additional analytic analysis is possible for estimating hole volume and penetration cavity profiles using the work of Murphy, et al. [6,7]. The references provide a basis for quantifying the energy per unit volume of target removed for a variety of materials. The volume, **V,** of target material removed was found to be directly proportional to the jet energy, $\mathbf{V} = E/c$, with c being a constant in the most basic application of the model. The observation that penetrator material was only a second order effect on hole volume reinforces the utility of this paper's 1-D analysis. More complicated forms, including that of Perez [8] and Szendrei [9] can be applied; but at the hypervelocity regime of the shaped charge jet, then the approximation of a fixed constant is suitable. The constant proportionality between jet energy deposited and target volume removed is seen in the Figure 7, extracted from Ref. [6].
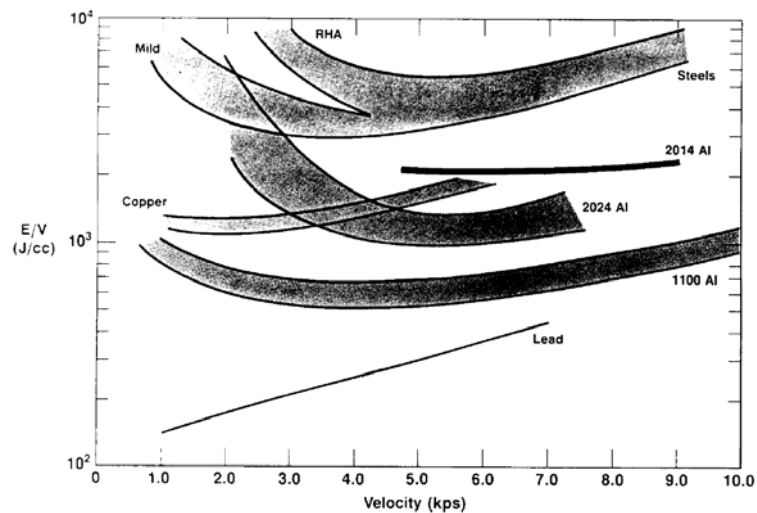

Fig. 7. Energy-hole volume removed from Ref. [6] for various materials

Murphy's relations are easily incorporated into the differential form of the energy relationships to give the form of Eq. (16). Values of the proportionality constant, c, are found in Figure 7 for common metals and in Table 1 for some geologic materials and can be directly applied in such analysis.

$$\frac{d\mathbf{V}}{dp} = \frac{dE}{dp}\left(\frac{d\mathbf{V}}{dE}\right)_{Ref\,6} \quad \text{with} \quad \frac{d\mathbf{V}}{dE} \approx \frac{1}{c} \tag{16}$$

Table 1. Energy per unit volume constant for various geologic materials Ref.[10]

Target Material	c (J/cc)
Concrete	882
Limestone	1976
Granite	2409

3.   MATERIAL BACKFLOW

The final discussion is of the impact, material backflow, and interface velocities given back in Figure 1. This is a departure from the energy-volume relations just discussed, but is relevant to the 1-D analysis originally posed. Staying in the coordinate system fixed to the interface, the ratio of backflow material (i.e. material turned from the interface impact) to the impact velocity is studied. That ratio is,

$$\frac{V_{backflow}}{V_{impact}} = \frac{V - 2u}{V - u} = \frac{\gamma - 1}{\gamma} \tag{17}$$

This ratio delineates the penetrator/target combinations where the backflow transitions from a rebounding (opposite direction to the incoming penetrator) interaction to an incoming (same direction as the penetrator). Recall that this is with respect to a reference system attached to the moving interface. The works of Allen and Rogers [11] describes a 'secondary penetration' that may occur and the relationship of Eq. (17) and the following discussion compliment their hypothesis.

The response curves of the backflow-impact velocity ratio are shown in Fig. 8 for penetrator material densities impacting various target densities. The transition points (i.e. material is leaving the interface at the same rate as the incoming penetrator) are at the expected values where the impactor and target are of identical density. The response curves also support the phenomenon commonly observed in experiments having high density, ductile metals (e.g. tantalum) penetrating lower density targets (e.g. Al or steel) where, for specific velocities and sufficient target depth, the penetrator is recovered as a 'thimble' or inverted cylinder, yet totally intact as in Figure 9. The negative-valued domain of Figure 8 has the backflow material moving in the same direction, albeit lower in magnitude, as the incoming penetrator. The unique condition of post-recovery of a fully inverted cylinder also requires material ductility and flow stress to turn along the streamline, as well as have sufficient strength to resist the strain and retard the gradient along the inverted penetrator.
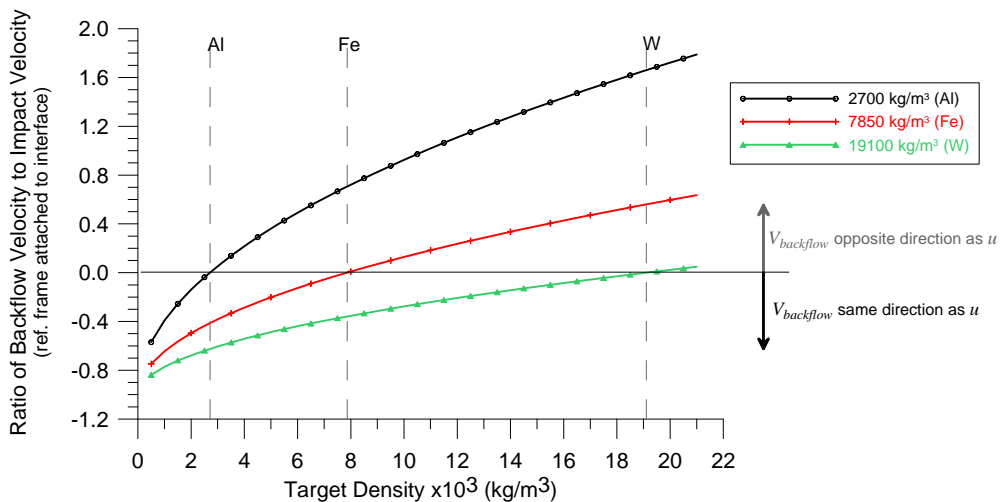

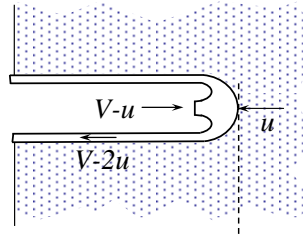Fig. 8. Backflow velocity response curves

Fig. 9. Diagram of the inverting cylinder during penetration

The sign of the ratio also dictates the momentum and energy exchange to the penetration interface. This was quantified in the earlier presentation of spatial energy and momentum deposition terms and graphs. Penetrators of low density (with respect to the target density) have greater efficiency on the momentum and energy exchange with an analogy made to perfectly elastic and perfectly plastic impacts in rigid body dynamics studies.

4. CONCLUSIONS

In this paper, a one-dimensional analysis of fundamental penetration was made with relationships that characterize the energy and momentum input as a function of material densities. These relationships are useful in the understanding of the effect of material density and the ability to tailor or dictate desired penetration goals. Low density penetrators deposit a greater percentage of their energy in the initial phase, while the higher density materials carry their energy deeper within the target. An example a shaped charge jet penetration of a severely over-matched target was used to illustrate how control of energy deposition might be exploited. By matching penetrator density to target density, the momentum, energy and power relationships can be used to guide first-order objectives.

The analysis is ideally suited for applying energy versus hole volume data and models from the research database. Estimates for hole profiles can be directly obtained knowing initial characteristics of rod and shaped charge jet penetrators along with the analytic equations presented. Material strength and complex penetrator/target interactions were not addressed, herein, but should be considered for regimes outside of the hydrodynamic, incompressible, and inviscid domain of this derivation.

Further discussions were made on the interfacial velocity and the relative nature of the reverse streamline, or backflow. The relationship should be considered in the fundamental understanding of the penetration process and how one might be able to exploit this process through material selection. These relations are a useful addition to the abundance of subject matter that exists relating to high and hypervelocity penetration.

ACKNOWLEDGMENTS

REFERENCES

[1]   Birkhoff G, MacDougall D, Pugh E, Taylor G. Explosives with lined cavities. *J. Appl. Phys*., 1948; **19**(6).

[2]   Pugh E. A Theory of target penetration of jets. National Defense Research Committee Armor and Ordnance, Report No. A-274 (OSRD No. 3752) Division 2, June 1944.

[3]   Foster JC, Wilson LL. Energy and momentum considerations for high velocity penetration processes. *Proc. 17th Southeastern Conf. on Theor. and Appl. Mech. (SECTAM-XVII*), Hot Springs AR, 1994.

[4]   Foster JC, Mayersak JR. Terminal ballistics of hypervelocity shaped charge devices. *Proc. 2nd Ballistics Symposium on Classified Topics*, Applied Physics Laboratory, Johns Hopkins Univ., Laurel, MD, 27-29 Oct 1992.

[5]   Allison FE, Bryan GM. Cratering by a train of hypervelocity fragments. *Proc. 2nd Hypervelocity Impact Effects Symp*. 1957; **1**: 81.

[6]   Murphy MJ. Survey of the influence of velocity and material on the projectile energy/target hole volume relationship. *Proc. 10th Int'l Symp. on Ballistics*, San Diego, CA, 1987.

[7]   Murphy MJ, Henderson JM. Computer simulation of concrete penetration by shaped charge jets. *Proc. 7th Int'l Symp. on Ballistics*, The Hague, Netherlands, 1983.

[8]   Perez E. A theory for armor penetration by hypervelocity long rod. *Proc. 4th Int'l Symp. on Ballistics*, 1978.

[9]   Szendrei T. Analytical model of crater formation by jet impact and its application to calculation of penetration curves and hole profiles. Proc. 7th Int'l Symp. on Ballistics*, The Hague, Netherlands, 1983.

[10] Murphy MJ, Kuklo RM, Rambur TA, Switzer LL, Summer MA. Single and multiple jet penetration experiments into geologic materials. Department of Energy Report, UCRL-CONF-201680.

[11] Allen WA, Rogers, JW. Penetration of a rod into a semi-infinite target. Franklin Institute, 1961; **272**(4): 275-284.